Journal of Sound and Vibration (2000) **232**(3), 541–551
doi:10.1006/jsvi.1999.2769, available online at http://www.idealibrary.com on IDEAL®

VIBRATION CONTROL OF A ROTATING EULER–BERNOULLI BEAM

H. DIKEN

Faculty of Aeronautics and Astronautics, Istanbul Technical University, 80626 *Maslak, Istanbul, Turkey*

(*Received* 18 *November* 1998, *and in final form* 26 *October* 1999)

In this paper, vibration control of a rotating Euler–Bernoulli beam is considered. It is assumed that the fixed–free elastic beam is attached to the servomotor which uses PD control to achieve the desired angular rotation, at the same time, the shear force measured at the root of the beam is used as a feedback to control the beam tip vibration. Mode summation techniques and Laplace domain synthesis techniques are used to analyze the system. Parametric transfer functions relating beam tip motion to the desired rotation and beam rotation to the desired input rotation are obtained. One parameter is the frequency ratio between the natural frequency of the beam and the frequency of the control system, second parameter is the ratio between the shear force feedback gain and the control damping. Stability conditions with respect to these parameters are given. The effect of these parameters on the rotational motion and the beam tip vibration is discussed. Some values of these parameters that make possible desired rotational motion with suppressed tip vibration are suggested. Analysis and results of this work can also be applied to the bending strain feedback and tip velocity feedback control of a rotating Euler–Bernoulli beam.

1. INTRODUCTION

Recently, the problem of modelling and control of a rotating flexible beam has received wide-spread attention in connection with the applications like flexible robot arms, rotor blades and spacecraft with flexible appendages. Most of the studies have used Euler–Bernoulli beam theory in their model. A review regarding modelling, design and control of an Euler–Bernoulli beam-type manipulator has been presented by Book [1]. The pinned–free Euler–Bernoulli beam with distributed sensors to investigate the generic properties of the structural modelling pertinent to the structural control is studied by Spector and Flasher [2]. Point-to-point position control of a flexible rotating beam is performed by using Laplace domain synthesis techniques by Bhat *et al.* [3, 4]. Dynamic modelling and optimal control of a rotating Euler–Bernoulli beam is studied by Zhu and Mote [5]. A rotating Euler–Bernoulli beam with the dynamic boundary force and moment applied at the tip of the beam was studied for the stability of the control by Morgul [6]. Recently, rotating Timoshenko beam equations for pinned–free and clamped–free cases have been developed in the work of White and Heppler [7]. The rotating Timoshenko beam with tip payload, including the effect of stiffening is studied by Yuan and Hu [8]. In their study, to achieve joint angle trajectory tracking with simultaneous suppression of elastic vibrations, a non-linear controller was designed using input–output linearization and elastic mode stabilization. Recently, a rotating Euler–Bernoulli beam with shear force feedback control was investigated by Luo and Guo [9]. The primary concern was the

0022-460X/00/180541 + 11 $35.00/0

stability analysis of the closed-loop equation. Some experiments were also conducted to verify the analysis. To keep consistency with the theoretical discussions only vibration suppression is considered, but the motor angular position control is ignored.

In this paper a rotating Euler–Bernoulli beam is considered as a dynamical system. Shear force feedback is used to suppress the beam tip vibration. In addition to the work done by Luo and Guo [9] rotational control of the beam is added. Mode summation techniques and Laplace domain synthesis techniques are used to analyze the system. Parametric transfer functions relating the tip motion to the desired rotation and also the beam rotation to the desired rotation are obtained. One parameter is the frequency ratio between the natural frequency of the beam and the frequency of the control system. A second parameter is the ratio between the shear force feedback gain and the control damping. Stability conditions are obtained with respect to these parameters.

2. MODELLING

Derivation of the equations of the dynamic model, which is a rotating Euler–Bernoulli beam under fixed–free boundary conditions will not be discussed here; details can be found in references [7, 8]. They have used Timoshenko beam theory which takes into account the effect of shear, by neglecting shear, the equations will be reduced to the one for the Euler–Bernoulli beam. The governing equations of the dynamic system are

$$EIw^{iv} + m\ddot{w} = -mx\ddot{\theta}, \tag{1}$$

$$J_{tot}\ddot{\theta} + \int_0^l m\ddot{w}x\,\mathrm{d}x = \tau, \qquad J_{tot} = \frac{J_m}{n^2} + J_b. \tag{2}$$

Here E is the modulus of elasticity, I is the area moment of inertia of the beam cross-section, w is the beam deflection measured with respect to the rotating frame, l is the length of the beam, m is the mass per unit length, θ is the rotational angle, J_{tot} is the total mass moment of inertia with respect to the beam axis which includes the motor inertia J_m and the beam inertia J_b, n is the gear ratio between the beam rotational angle and the motor rotational angle, τ is the motor torque with respect to the beam axis. The sum of the orthogonal modes is assumed as the solution to the equation (1) [11];

$$w(t, x) = \sum_{i=1}^{n} \phi_i(x) q_i(t). \tag{3}$$

Here $\phi_i(x)$ is ith orthogonal mode, $q_i(t)$ is the ith generalized co-ordinate. The characteristic equation and also the ith orthogonal mode of the fixed–free beam can be given as

$$\cosh\beta_i l \cos\beta_i l + 1 = 0, \qquad (\beta_i l)^2 = \sqrt{\frac{ml^4}{EI}}\,\omega_i \tag{4}$$

$$\phi_i(x) = C\left[\cosh\beta_i x + \cos\beta_i x - \frac{\sinh\beta_i l - \sin\beta_i l}{\cosh\beta_i l + \cos\beta_i l}\sinh\beta_i x - \sin\beta_i x)\right]. \tag{5}$$

Here ω_i is the ith natural frequency of the beam. After substituting the assumed solution into equation (1) and using orthogonality conditions, the following equation for the

generalized co-ordinates can be obtained as:

$$\ddot{q}_i + \omega_i^2 q_i = -l\alpha_i \ddot{\theta}, \qquad \alpha_i = \frac{\int_0^1 \phi_i(\xi)\,\mathrm{d}\xi}{\int_0^1 \phi_i^2(\xi)\,\mathrm{d}\xi}, \qquad \omega_i = (\beta_i l)^2 \sqrt{\frac{EI}{ml^4}}, \qquad \xi = \frac{x}{l}, \tag{6}$$

where α_i is the mode participation factor. After taking Laplace transform of equation (6) the resulting equation is

$$(s^2 + \omega_i^2)\bar{Q}_i(s) + s^2\theta(s) = 0, \qquad \bar{Q}_i(s) = \frac{Q_i(s)}{l\alpha_i}, \tag{7}$$

By using the solution given in equation (3) the following equation is obtained for equation (2):

$$\ddot{\theta} + \sum_{i=1}^{n} \eta_i \ddot{\bar{q}}_i = \frac{\tau}{J_{tot}}, \qquad \eta_i = \frac{3\alpha_i \int_0^1 \phi_i(\xi)\,\mathrm{d}\xi}{1 + (J_m/n^2)/J_b}, \qquad \bar{q}_i = \frac{q_i}{l\alpha_i}, \qquad J_b = \frac{ml^3}{3}. \tag{8}$$

Here the beam is assumed to be uniform and rectangular. If the ratio between J_m/n^2 and J_b is assumed equal to one, η values for the first three natural frequencies of the fixed–free flexible beam are $\eta_1 = 0{\cdot}4853$, $\eta_2 = 0{\cdot}0124$, $\eta_3 = 0{\cdot}0016$. Figure 1 shows the block diagram of the servomotor control system with the shear force feedback. From the diagram we can obtain the Laplace transform of torque with respect to the beam axis as

$$T(s) = \frac{K_T}{n^2 R_0}\left[[\theta_d(s) - \theta(s)](K_p + sK_d) - sK_b\theta(s) + sK\sum_{i=1}^{n} \phi_i''(0) l\alpha_i \bar{Q}_i(s)\right]. \tag{9}$$

Here K_T is the torque constant, R_a is the armature coil resistance, θ_d is the desired angular input, K_p is the proportional gain, K_d is the derivative gain, K_b is the electromotive force constant, and K is the shear force feedback gain. Generally, the armature coil inductance L_a is much smaller than the armature coil resistance R_a, that is why it is neglected. For the time being, the solution is assumed for the first natural frequency of the beam, that is, $i = 1$. If we take Laplace transform of equation (8) and use equation (9), the resulting equation is

$$(\eta_1 s^2 - \bar{K}_1 s)\bar{Q}_1(s) + [s^2 + (\bar{K}_d + \bar{K}_m)s + \bar{K}_p]\theta(s) = (\bar{K}_p + s\bar{K}_d)\theta_d(s). \tag{10}$$

Here the shear force feedback gain K, the proportional gain K_p and the derivative gain K_d are redefined as

$$\bar{K}_1 = l\alpha_1 \phi_1''(0)\frac{K_T K}{n^2 J_{tot} R_a}, \qquad \bar{K}_p = \frac{K_T K_p}{n^2 J_{tot} R_a},$$

$$\bar{K}_d = \frac{K_T K_d}{n^2 J_{tot} R_a}, \qquad \bar{K}_m = \frac{K_T K_b}{n^2 J_{tot} R_a}, \tag{11}$$

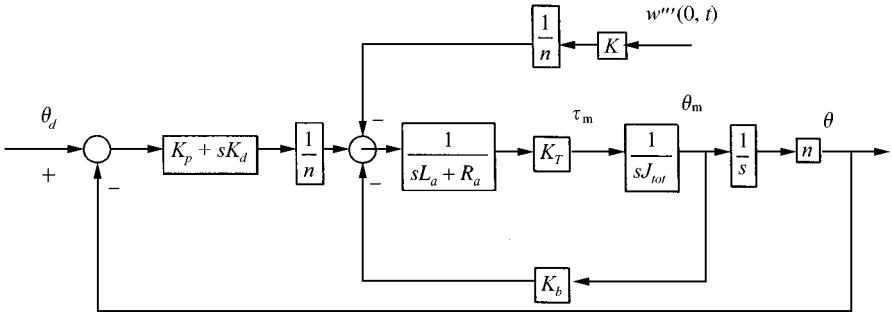

Figure 1. Block diagram of the servomotor control with shear force feedback.

where $\bar{K}_m$ is the motor time constant. Now, one can write the Laplace transform of the differential equations in matrix form given in equations (7) and (10) as

$$\begin{bmatrix} s^2 + (\bar{K}_d + \bar{K}_m)s + \bar{K}_p & \eta_1 s^2 - \bar{K}_1 s \\ s^2 & s^2 + \omega_1^2 \end{bmatrix} \begin{bmatrix} \theta(s) \\ \bar{Q}_i(s) \end{bmatrix} = \begin{bmatrix} \bar{K}_p + \bar{K}_d s \\ 0 \end{bmatrix} \theta_d(s). \tag{12}$$

From equation (12) one can derive the transfer functions relating the beam tip motion to the desired rotation and the beam rotation to the desired rotation as follows:

$$\frac{\bar{Q}_1(s)}{\theta_d(s)} = \frac{-\bar{s}^2(2\zeta\bar{s} + 1)}{(1 - \eta_1)\bar{s}^4 + 2\zeta(1 + \gamma_1)\bar{s}^3 + (\rho_1^2 + 1)\bar{s}^2 + 2\zeta\rho_1^2\bar{s} + \rho_1^2}, \tag{13}$$

$$\frac{\theta(s)}{\theta_d(s)} = \frac{(\bar{s}^2 + \rho_1^2)(2\zeta\bar{s} + 1)}{(1 - \eta_1)\bar{s}^4 + 2\zeta(1 + \gamma_1)\bar{s}^3 + (\rho_1^2 + 1)\bar{s}^2 + 2\zeta\rho_1^2\bar{s} + \rho_1^2}, \tag{14}$$

$$\rho_1 = \frac{\omega_1}{\omega}, \qquad 2\zeta\omega = \bar{K}_d + \bar{K}_m, \qquad \omega^2 = \bar{K}_p, \qquad \frac{\bar{K}_p}{\bar{K}_d} = \frac{\omega^2}{2\zeta\omega - \bar{K}_m} = \frac{\omega}{2\zeta - (\bar{K}_m/\omega)} \approx \frac{\omega}{2\zeta} \tag{15}$$

$$2\zeta_1\omega = \bar{K}_1, \qquad \gamma_1 = \frac{\zeta_1}{\zeta}, \qquad \bar{s} = \frac{s}{\omega}, \tag{16}$$

Generally, motor time constant $\bar{K}_m$ is much smaller than the control frequency ω, so the ratio $\bar{K}_m/\omega$ will be much smaller than 2ζ and can be ignored. Here ρ_i is the frequency ratio, ω_1 is the first natural frequency of the beam, ω is the control system frequency, ζ is the control system damping, ζ_1 is defined as the damping ratio for the shear force feedback, and γ_1 is the ratio between these dampings.

3. ROOT LOCUS ANALYSIS

In the proceeding root locus analysis, the effect of η will be neglected and considered later. To see the effect of the frequency ratio ρ_1 on the poles of the system, let us rearrange the denominator of the transfer function or the characteristic equation of the control system

given either in equations (13) or (14) such as

$$\bar{s}^2[\bar{s}^2 + 2\zeta(1+\gamma_1)\bar{s} + 1] + \rho_1^2[\bar{s}^2 + 2\zeta\bar{s} + 1] = 0. \tag{17}$$

When $\rho_1 = 0$, roots start at the poles,

$$\bar{p}_{1,2} = 0, \qquad \bar{p}_{3,4} = -\zeta(1+\gamma_1) \mp \sqrt{1-\zeta^2(1+\gamma_1)^2}\,\mathrm{j} \tag{18}$$

and when $\rho_1 = \infty$, they end at the zeros,

$$\bar{z}_{1,2} = -\zeta \mp \sqrt{1-\zeta^2}\,\mathrm{j}, \tag{19}$$

In fact, these zeros are the rigid control system poles. Root loci of equation (17) are shown in Figures 2–4. Plots are drawn for $\zeta = 0{\cdot}3$, $0{\cdot}5$, and $0{\cdot}7$ respectively. In each figure, root loci are also drawn for the three different values of γ_1, namely, $\gamma_1 < \gamma_b$, $\gamma_1 = \gamma_b$, and $\gamma_1 > \gamma_b$. γ_b is a kind of boundary value which is equal to

$$\gamma_b = \frac{\zeta}{1-\zeta}. \tag{20}$$

When $\gamma_1 < \gamma_b$, one pair of branches starts from the poles $\bar{p}_{1,2}$ and go to infinity, the other branches start from the poles $\bar{p}_{3,4}$ and end at the zeros. When $\gamma_1 > \gamma_b$, branches starting from $\bar{p}_{1,2}$ this time go to $\bar{z}_{1,2}$ instead of infinity. When $\gamma_1 = \gamma_b$, branches coming from $\bar{p}_{1,2}$ and $\bar{p}_{3,4}$ have junction point at which all four roots are equal to each other. At this junction point, ρ_1 has the value of

$$\rho_b = \frac{1}{1-\zeta} \tag{21}$$

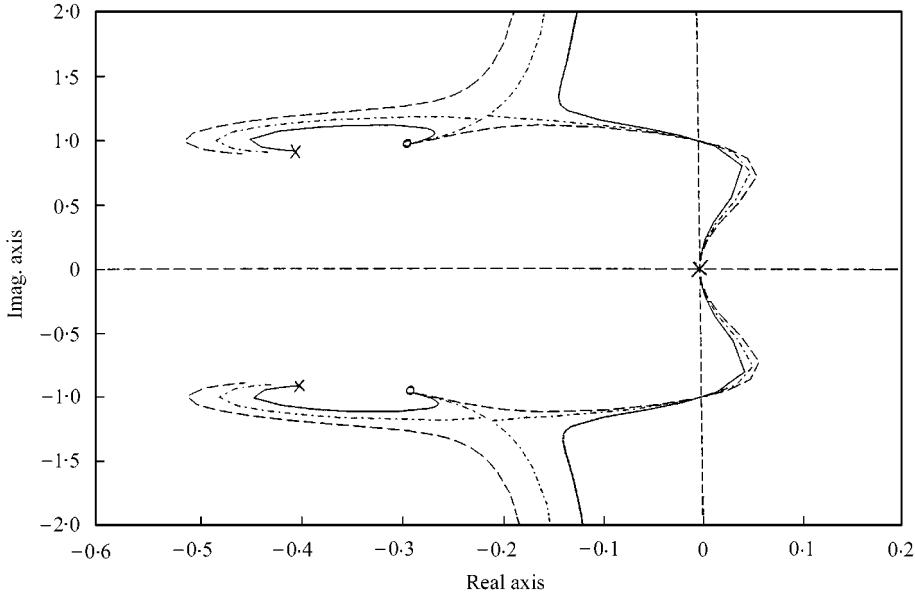

Figure 2. Root loci with respect to ρ_1: $\zeta = 0{\cdot}3$, ——: $\gamma_1 < \gamma_b$; −·−·−: $\gamma_1 = \gamma_b$; – – –: $\gamma_1 > \gamma_b$.

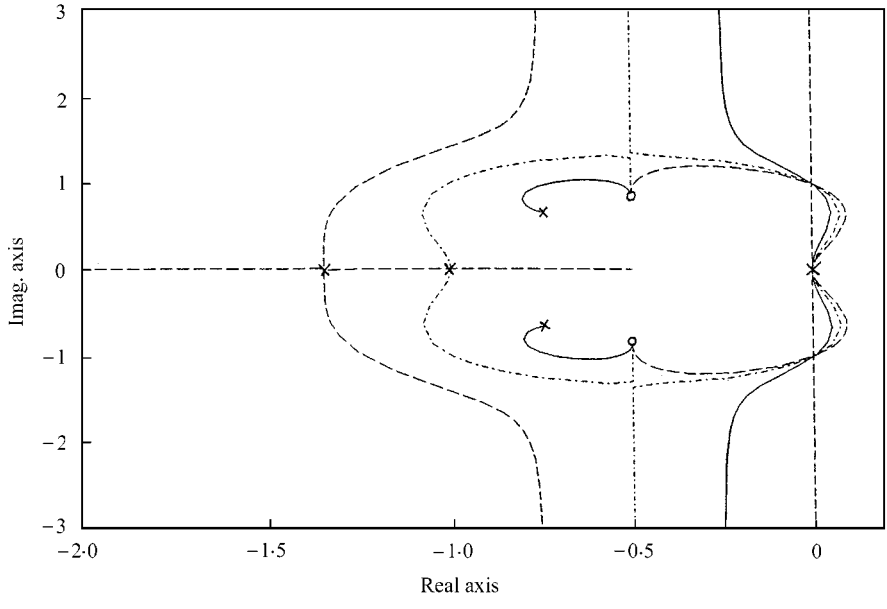

Figure 3. Root loci with respect to ρ_1: $\zeta = 0{\cdot}5$, ——: $\gamma_1 < \gamma_b$; −·−·−: $\gamma_1 = \gamma_b$; − − −: $\gamma_1 > \gamma_b$.

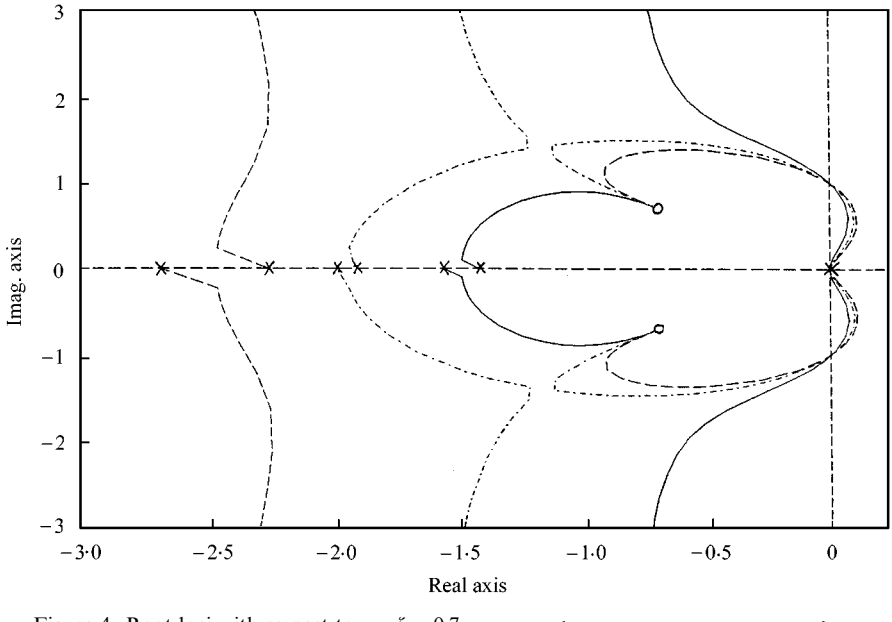

Figure 4. Root loci with respect to ρ_1: $\zeta = 0{\cdot}7$, ——: $\gamma_1 < \gamma_b$; −·−·−: $\gamma_1 = \gamma_b$; − − −: $\gamma_1 > \gamma_b$.

which is considered as a boundary value for ρ_1. The control damping $\zeta = 0{\cdot}5$ has also an effect on the branching. When $\zeta > 0{\cdot}5$, branches are inclined away from the imaginary axis, for the values of $\zeta < 0{\cdot}5$, branches are inclined toward the imaginary axis and at $\zeta = 0{\cdot}5$, branches are vertical and parallel to the imaginary axis.

Since one pair of the branches has a part which lies on the right side of the s plane, for some values of ρ_1 the system will be unstable. The critical value of ρ_1 at which the branch

crosses the imaginary axis is

$$\rho_{1cr} = \sqrt{1 + \gamma_1}. \tag{22}$$

Then, for a selected value of γ_1, in other words, for a selected value of the shear force feedback gain, the frequency ratio ρ_1 should be selected greater than ρ_{1cr} for the stability. If the value of ρ_1 is selected first, the stability condition with respect to γ_1 can also be derived as

$$0 \leqslant \gamma_1 \leqslant (\rho_1^2 - 1). \tag{23}$$

If η_1 is not neglected, stability conditions given with equations (22) and (23) can be approximated with the following equations:

$$\rho_{1cr} = \sqrt{\frac{1 + \gamma_1}{1 + \eta_1}}, \qquad 0 \leqslant \gamma_1 \leqslant [(1 + \eta_1)\rho_1^2 - 1]. \tag{24}$$

4. RESPONSE ANALYSIS

Figures 5 and 6 show the responses of the beam rotational motion and beam tip vibration to the step input respectively. The tip vibrational motion of the flexible beam is

$$\frac{w(l, t)}{l} = \sum_{i}^{n} \alpha_i \phi_i(l) \bar{q}_i(t), \tag{25}$$

The results are obtained only for the first mode, the effect of the other modes will be considered later. In the plots of Figures 5 and 6, control damping is chosen as $\zeta = 0{\cdot}7$. In

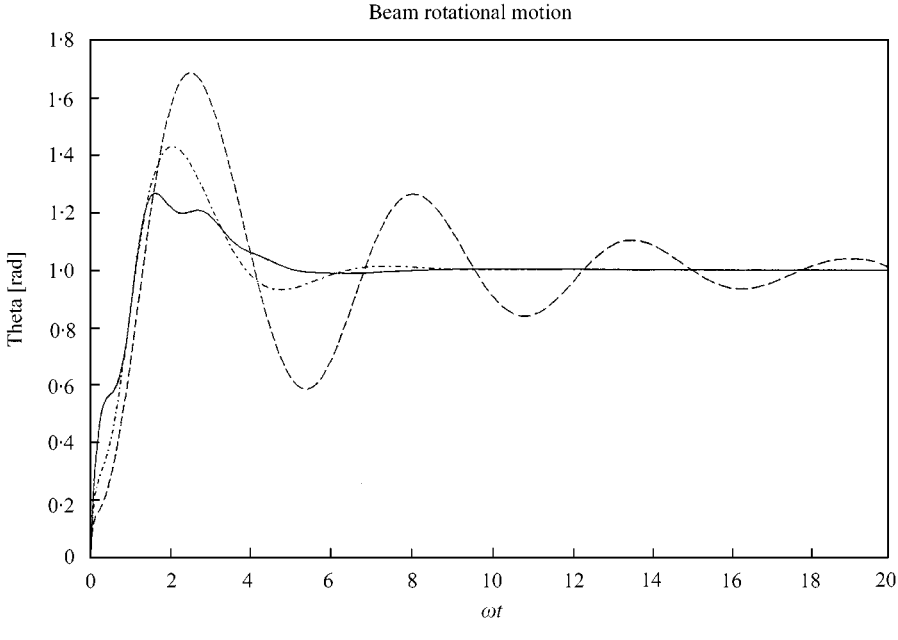

Figure 5. Step responses for the beam rotational motion: $\zeta = 0{\cdot}7$, $\rho_1 = \rho_b$, ——: $\gamma_1 = 0{\cdot}1\gamma_b$; – · – · –: $\gamma_1 = \gamma_b$; – – –: $\gamma_1 = 2{\cdot}5\gamma_b$.

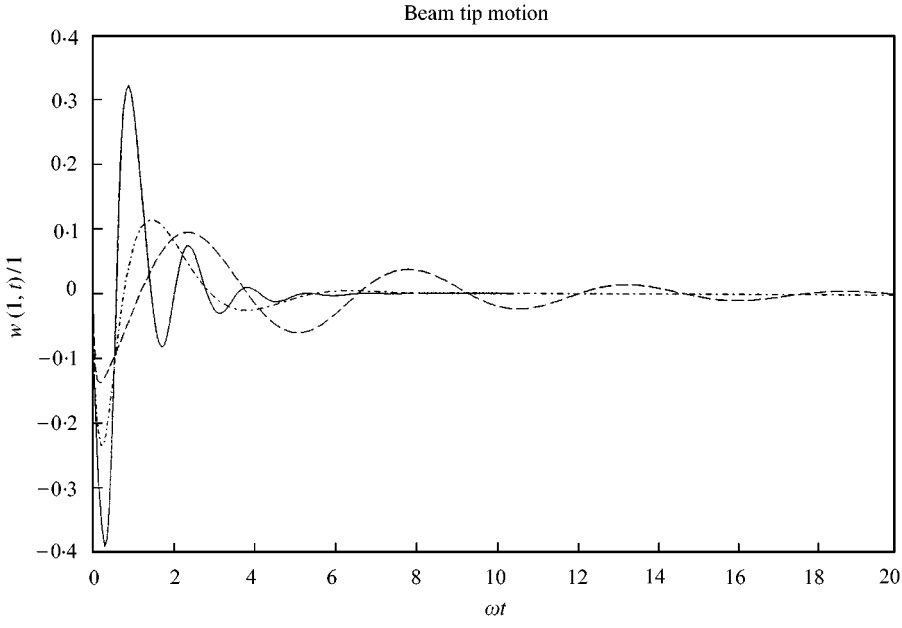

Figure 6. Step responses for the beam tip motion: $\zeta = 0{\cdot}7$, $\rho_1 = \rho_b$, ——: $\gamma_1 = 0{\cdot}1\gamma_b$; –·–·–: $\gamma_1 = \gamma_b$; – – –: $\gamma_1 = 2{\cdot}5\gamma_b$.

these plots while $\rho_1 = \rho_b = 3{\cdot}33$, γ_1 assumes three different values. For $\gamma_1 < \gamma_b = 2{\cdot}33$, one pair of roots is close to the rigid system poles, but the other pair of roots has low-damping and high-frequency component, hence the desired rotational motion is achieved but rippling occurred, and the beam tip has also lightly damped vibration. The rotor locus for this case is a solid line plot given in Figure 4. For $\gamma_1 = \gamma_b$, roots are complex; their values are close to the rigid system poles but with higher damping and frequency values and hence the higher overshoot is obtained. The root locus for this case is the dash-dot line plot given in Figure 4. For $\gamma_1 > \gamma_b$, one pair of roots is closer to the imaginary axis than the other ones and also have lower damping and higher frequency values than the rigid system poles, that is why rotational motion and also beam tip motion has lightly damped vibration. The root locus for this case is the dashed line plot given in Figure 4. Figures 7 and 8 show the step responses of the system for the case in which while $\gamma_1 = \gamma_b$, ρ_1 assumes different values. For $\rho_1 < \rho_b$, both the rotational motion and the beam tip motion has lightly damped vibration. For $\rho_1 = \rho_b$, response is close to that of the rigid system but overshoot is higher. For values of $\rho_1 > \rho_b$, the desired rotational motion is obtained, at the same time the beam tip vibration is quickly damped with low amplitudes. Practically, for

$$\rho_1 \geqslant 4\rho_b \quad \text{and} \quad \gamma_1 = \gamma_b \tag{26}$$

or

$$\omega_1 \geqslant \frac{4\omega}{1-\zeta} \quad \text{and} \quad \zeta_1 = \frac{\zeta^2}{1-\zeta}, \tag{27}$$

the desired rotational motion with suppressed beam tip vibration can be obtained. To see the effect of the other modes, the response to each individual mode can be calculated and

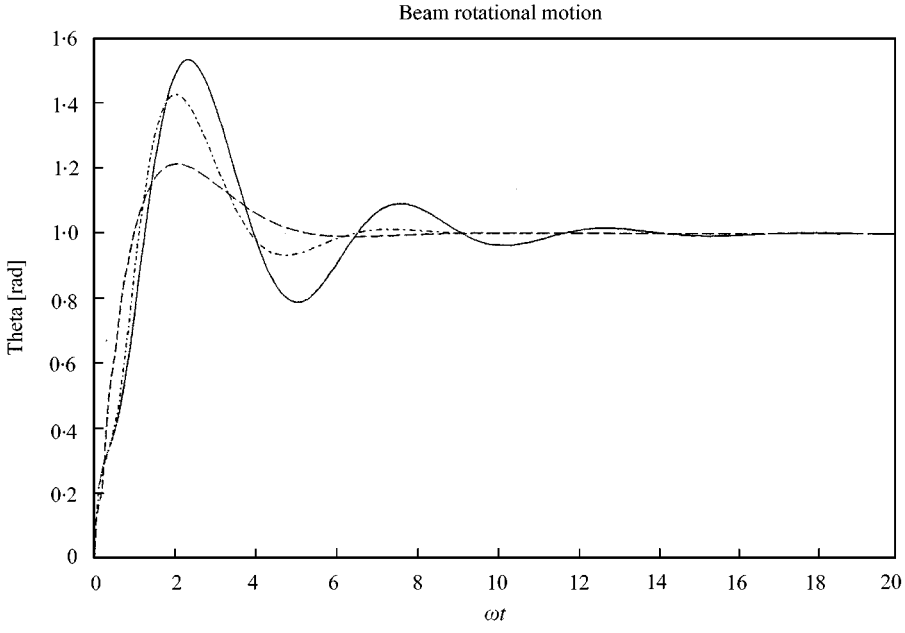

Figure 7. Step responses for the beam rotational motion. $\zeta = 0{\cdot}7$, $\gamma_1 = \gamma_b$, ——: $\rho_1 = 0{\cdot}8\rho_b$; – · – · –: $\rho_1 = \rho_b$; – – –: $\rho_1 = 4\rho_b$.

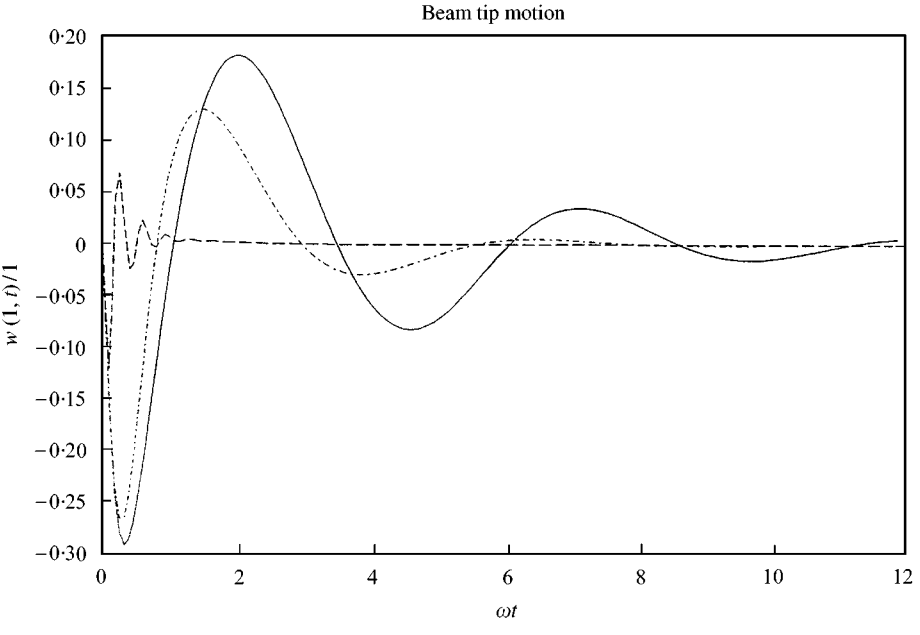

Figure 8. Step responses for the beam tip motion: $\zeta = 0{\cdot}7$, $\gamma_1 = \gamma_b$, ——: $\rho_1 = 0{\cdot}8\rho_b$; – · – · –: $\rho_1 = \rho_b$; – – –: $\rho_1 = 4\rho_b$.

summed up. For the second and third modes the following values should be used:

$$\rho_2 = \frac{\omega_2}{\omega_1}\rho_1 = 2{\cdot}5\rho_1, \quad \rho_3 = \frac{\omega_3}{\omega_1}\rho_1 = 4{\cdot}2\rho_1,$$

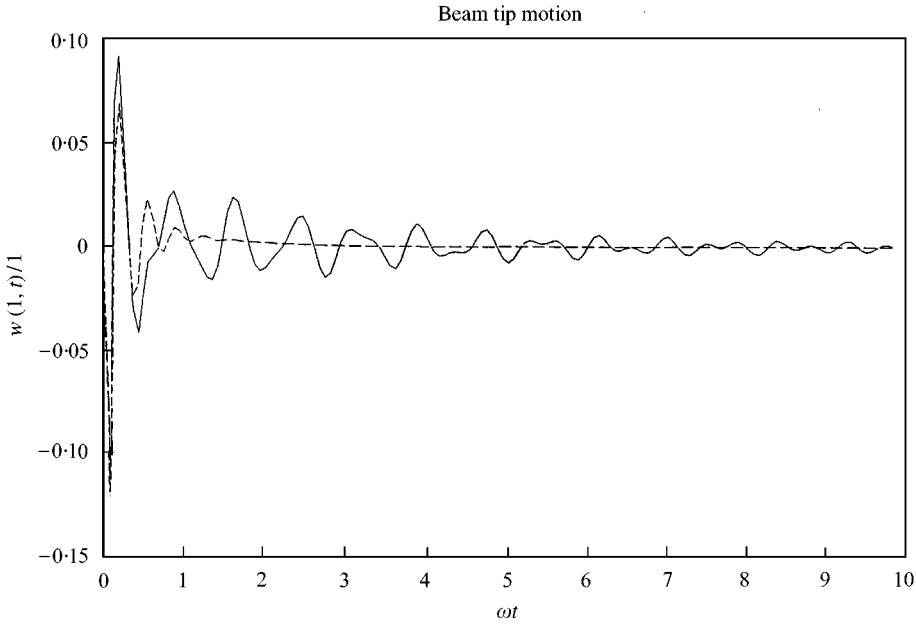

Figure 9. Step response of the beam tip motion: $\zeta = 0{\cdot}7$; $\rho_1 = 4\rho_b$; $\gamma_1 = \gamma_b$. '——' first three modes are considered; '– – –' only first mode is considered:

$$\gamma_2 = \frac{\alpha_2 \phi_2'''(0)}{\alpha_1 \phi_1'''(0)} \gamma_1 = 0{\cdot}2215\gamma_1, \qquad \gamma_3 = \frac{\alpha_3 \phi_3'''(0)}{\alpha_1 \phi_1'''(0)} \gamma_1 = 0{\cdot}0775\gamma_1. \tag{28}$$

Figure 9 shows the step response of the system in which the first three modes are considered. The effective mode is the first one as expected.

The foregoing analysis and results can also be used for the bending strain feedback, and also for the tip velocity feedback. Since the bending strain is proportional to $\dot{w}''(0, t)$ and the tip velocity is proportional to $\dot{w}(l, t)$, the definition of the gain constants will, respectively, be

$$\bar{K}_1 = l\alpha_1 \phi_1''(0) \frac{K_T K}{n^2 J_{tot} R_a}, \qquad \bar{K}_1 = l\alpha_1 \phi_1(l) \frac{K_T K}{n^2 J_{tot} R_a}. \tag{29}$$

The rest of the analysis remains same.

5. CONCLUSION

A servomotor-driven rotating elastic beam is modelled and analyzed. The beam is considered fixed-free and modelled as an Euler–Bernoulli beam. To achieve the desired angular motion, PD control, and to suppress the beam tip vibration, the shear force feedback is used. Mode summation techniques and Laplace domain synthesis techniques are used for the analysis. Parametric transfer functions relating the beam tip motion to the desired rotation, and the beam rotation to the desired rotation are obtained. One parameter is the frequency ratio between the natural frequency of the beam and the frequency of the control system, and the second parameter is the ratio between the shear force feedback gain and the control damping. The system becomes unstable for certain values of these

parameters. Conditions for the optimum control of the rotational motion as well as for suppressing beam tip vibrations are derived and given as a function of these parameters. Analysis and results are also equally valid for the bending strain feedback, and tip velocity feedback control of the rotating Euler–Bernoulli beam.

REFERENCES

1. W. J. Book 1990 *Proceedings of the 29th Conference on Decision and Control, Honolulu, Hawaii*, 500–506. Modeling, design, and control of flexible manipulator arm: a tutorial review.
2. V. A. Spector and H. Flashner 1990 *ASME Journal of Dynamic Systems, Measurements, and Control* **112**, 186–193. Modeling and design implications of noncolocated control in flexible systems.
3. S. P. Bhat, M. Tanaka and D. K. Miu 1991 *ASME Journal of Dynamic Systems, Measurements, and Control* **113**, 432–437. Experiments on point to point position control of a flexible beam using Laplace transform technique—Part I: open loop.
4. S. P. Bhat and D. K. Miu 1991 *ASME Journal of Dynamic Systems, Measurements, and Control* **113**, 438–443. Experiments on point to point position control of a flexible beam using Laplace transform technique—part II: closed loop.
5. W. D. Zhu and C. D. Mote 1997 *Journal of Dynamic Systems, Measurement and Control*, **119**, 802–808. Dynamic modeling and optimal control of rotating Euler–Bernoulli beams.
6. O. Morgul 1992 *IEEE Transactions on Automatic Control* **37**, 639–642. Dynamic boundary control of Euler–Bernoulli beam.
7. M. W. White and G. R. Heppler 1996 *ASME Journal of Vibration and Acoustics*, **118**, 607–613. Vibration of a rotating Timoshenko beam.
8. K. Yuan and C. M. Hu 1996 *ASME Journal of Dynamic Systems, Measurement, and Control* **118**, 75–83. Nonlinear modeling and partial linearizing control of a slewing Timoshenko beam.
9. Z. H. Luo and B. Z. Guo 1997 *IEEE Transactions on Automatic Control* **42**, 53–65. Shear force feedback control of a single link flexible robot with a revolute joint.
10. H. Diken 1996 *AIAA Journal of Guidance and Control* **19**, 715–718. Precise trajectory tracking control of elastic joint manipulator.
11. W. T. Thomson 1981 *Theory of Vibration with Applications*. Englewood Cliffs NJ: Prentice-Hall.